Turbulence Modification in Dilute Small-Particle-Laden Liquid Jets

R. N. Parthasarathy* and Yin-Heng Chan†
University of Oklahoma, Norman, Oklahoma 73019

Nomenclature

d = diameter of injector, 7.6 mm
r = radial distance from jet centerline
U = mean axial velocity
u = axial velocity fluctuation
v = radial velocity fluctuation
x = axial distance from injector exit

Subscript

c = centerline value

I. Introduction

OVER the years, numerous theoretical and experimental studies have been conducted on the subject of turbulence modification in particle-laden jets. There is considerable scatter in experimental measurements dealing with the direct effects of particles on the turbulence of the carrier fluid called turbulence modulation.[1] It has been hypothesized that particles whose diameters d_p are smaller than the length scale of the energy-containing eddies, l_e, result in a reduction in the fluid turbulence because of the drag force acting on the particles. Larger particles, on the other hand, create turbulence in their wakes, thus increasing the turbulence intensity of the carrier fluid. A compilation of some past experimental measurements[2] indicates that the presence of particles results in a reduction in the carrier fluid turbulence for $d_p/l_e < 0.1$, whereas addition is observed for values of the critical parameter larger than 0.1. The amount of change in the fluid turbulence intensity depends on other parameters, such as particle concentration, density ratio, flow Reynolds number, etc. A few recent studies[3–5] have been aimed at delineating turbulence modulation effects in a variety of configurations. In some of these studies (involving gas flows) the fluid turbulence in the transverse direction was attenuated more strongly than the axial turbulence. Measurements highlighting the effects of small particles on the turbulence of liquid jets are particularly important because such particles are used as seed particles. The objective of this study was to determine the effects of small particles (64 and 180 μm in diameter) on fluid turbulence in a round water jet using a two-channel discriminator laser Doppler velocimeter (DLDV). First, a description of the experimental setup and instrumentation is given. Detailed results are presented next; the paper ends with the summary and significant conclusions.

II. Experimental Methods

Mixtures of glass beads and water were injected vertically downward in initially still water contained in a tank measuring $0.8 \times 0.8 \times 2.0$ m high. The tank was constructed with glass plates of 9.5-mm thickness on four sides to provide optical access to the flow. Filtered water was supplied at known flow rates to the injector by a rotary gear pump. A bypass valve and a filter accumulator were used to control and smoothen the flow. A standpipe was used to return the overflow water to a reservoir at the inlet of the pump. The tank dimensions were designed such that the effects of the return flow were small. The glass beads were fed by a variable-speed screw feeder (AccuRate Model 302) to a hopper tank and mixed with water before entering the injector flow through an eductor. The injector nozzle had an exit diameter of 7.5 mm with a contraction ratio of 12:1 and was designed to provide a uniform exit velocity profile, which was verified by LDV measurements.[6] The injector could be traversed vertically and laterally; lateral motion was achieved with a Unislide system, and vertical positioning was performed by a twin-screw mechanism. The test conditions, particle properties, and some flow properties are summarized in Table 1.

Five flows, including a single-phase (pure water) jet to serve as a baseline and four particle-laden jets having different particle sizes and loading, were studied. The flows were reasonably turbulent, all with an initial jet exit Reynolds number of approximately 9×10^3. The particles were Microbeads® Engineering Grade Class IV solid glass spheres supplied by Cataphote, Inc., with a material density of 2450 kg/m^3. The large glass beads (Type 710) were in the range of 149–210 μm with a mean diameter of 180 μm, whereas the small beads (Type 2027) ranged between 53 and 74 μm with a mean diameter of 64 μm. Both sets contained not more than 15% irregularly shaped particles, as specified by the manufacturer.

A TSI two-beam frequency-shifted on-axis forward-scatter LDV system based on a Lexel (Model 95) 2.5-W argon ion laser was used to measure the axial and radial velocities of the jet simultaneously. The measuring volumes were 0.16 mm in diameter and 2 mm long; the fringe spacings were 3.62 and 3.41 μm for the blue and green channels, respectively. The signals were processed using two Model 1980 (TSI, Inc.) burst-counter signal processors. Proper distinction between fluid and particle signals was achieved using a discriminator system[7,8] consisting of a laser beam from a 5-mW helium–neon laser, receiving optics, and an additional photomultiplier. When valid measurements from both channels were within the specified time window (50 μs), they were recorded digitally together with the discriminator voltage on a personal computer using a DataLink Multichannel Interface (TSI Model DL 100). During data analysis, a predetermined cutoff discriminator voltage was used to eliminate velocity measurements accompanied by a strong discriminator voltage. The remaining data were then refined (limited to those falling within ± 3 standard deviations) and statistically analyzed.

The operation of the LDV system was verified by measuring the velocity of the edge of a rotating disk and comparing it with measurements obtained from a stroboscope. Frequency shifting was used to eliminate errors due to directional ambiguity and bias. Concentration bias error was not significant in this study because the water used was seeded uniformly. The velocity measurements in the present study were number averaged; based on other studies in similar configurations,[9] it is assumed that the velocity bias errors were small. Also, the aim here is to compare the levels of turbulence among the various particle-laden jets; therefore, all of the measurements were number averaged for consistency. The gradient bias errors in the mean and fluctuating velocities throughout the jet were less than 1%. Thus, the overall bias errors in the LDV measurements of the liquid velocities were small for the present test conditions. The precision errors were computed using standard methods. The overall experimental uncertainties, evaluated at 95% confidence level, were as follows: mean and rms velocities, less than 7%, respectively, and turbulent kinetic energy, less than 13%.

III. Results

Measurements were first made in a water jet with no particles and were compared with existing single-phase turbulent jets. It was found that the mean and turbulent velocity statistics compared favorably with other measurements in turbulent self-similar jets.[6] Also, the measured mean velocity profiles for all of the particle-laden test conditions did not show any significant differences from the single-phase mean velocity profile, which indicated that the effects of particles on the mean velocity profile were negligible. Only the measurements highlighting the turbulence modulation effects of particles are presented here.

The normalized axial velocity fluctuations are plotted in Fig. 1. The solid line represents the curve fit of LDV data from Hussein et al.[10] for the fully developed single-phase turbulent jet (air-in-air) for an x/d range of 30–100 and a jet exit Reynolds number of 9.55×10^4. The axial turbulence intensity measurements for all the cases compare well with the measurements of Hussein et al.[10] and the single-phase measurements within experimental uncertainties;

Received 26 July 1999; revision received 10 August 2000; accepted for publication 18 September 2000.

*Associate Professor, School of Aerospace and Mechanical Engineering, 212 Felgar Hall, 865 Asp Avenue; rparthasarathy@ou.edu.

†Graduate Research Assistant, School of Aerospace and Mechanical Engineering, 212 Felgar Hall, 865 Asp Avenue.

Table 1 Summary of test conditions

Flow	Single-phase water jet	Particle-laden jet			
		Case 1	Case 2	Case 3	Case 4
Particle type	——	710	710	2027	2027
Particle size, μm	——	64	64	180	180
Particle terminal velocity, mm/s[a]	——	3	3	19	19
Particle time constant, ms[a]	——	0.55	0.55	3.2	3.2
Water flow rate, ml/s	63.08	63.08	63.08	63.08	63.08
Mass loading ratio ϕ_0, %[b]	0	1.1	2.3	1.1	2.3
Particle volume fraction, %	0	0.46	0.93	0.46	0.93
Initial average velocity, m/s	1.37[c]	1.34[c]	1.37[c]	1.43[d]	1.43[d]
Jet Reynolds number[e]	9174	8973	9107	9576	9576
Particle Stokes number[f]	——	0.0014	0.0014	0.008	0.008
Kolmogorov length scale, μm[f]	150	150	150	150	150
Kolmogorov length scale, ms[f]	22	22	22	22	22

[a]Computed values.
[b]Mass of particles per unit mass of water.
[c]Average injector exit velocity measured by LDV system at a distance of 2 mm (approximate) downstream from exit.
[d]Calculated from indicated volume flow rate.
[e]Values computed using injector exit diameter and injector exit velocity.
[f]Properties estimated based on the centerline values at $x/d = 60$ of the single-phase jet.

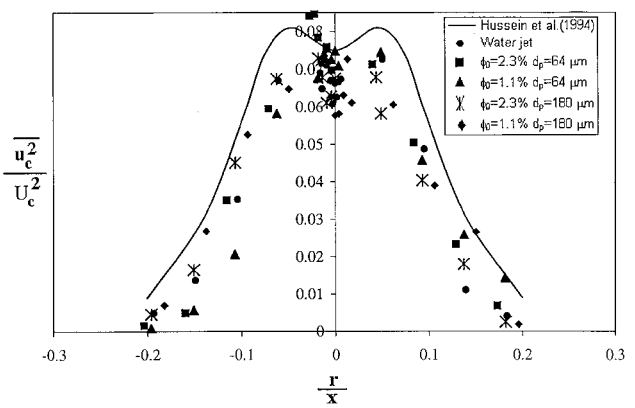

Fig. 1 Measured normalized streamwise velocity fluctuation profiles at 60 injector diameters downstream of the exit.

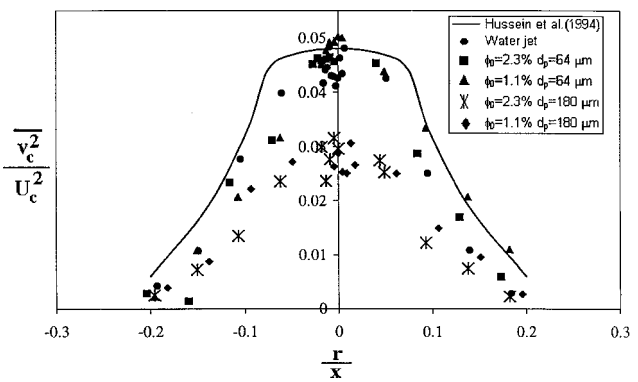

Fig. 2 Measured normalized radial velocity fluctuation profiles at 60 injector diameters downstream of the exit.

thus, it appears that the presence of particles at these loading levels did not affect the axial velocity fluctuations significantly. The radial turbulence intensity measurements of the particle-laden and single-phase jets are shown in Fig. 2. The measurements for the single-phase jet agree well with those of Hussein et al.[10] The radial velocity fluctuation measurements in the jets laden with the 64-μm particles are close to the single-phase measurements. However, the measurements in the 180-μm particle-laden jets display a significant reduction; the maximum radial turbulence intensity is approximately 30% lower than the corresponding single-phase value.

The terminal velocity of both particle sizes (3 and 19 mm/s) is small compared to the mean centerline velocity (140 mm/s); thus, particles of both sizes have negligible mean slip velocity. Also, the particle stokes numbers are small (0.0014 and 0.008), indicating that the particle time constants are small compared to the characteristic eddy timescale. The 64-μm particles are smaller than the Kolmogorov length scale at the jet centerline with a time constant of 2.5% of the Kolmogorov timescale. The 180-μm particles are comparable to the Kolmogorv length scale at the centerline; their time constant is 15% of the Kolmogorov timescale.

Thus, it is seen that the 64-μm particles are small enough to follow both the high and low frequencies of the velocity fluctuations; these particles can be used as tracer particles that follow the fluid motion faithfully. The time constant of the 180-μm glass beads corresponds to a frequency of 300 Hz. These particles are, therefore, not responsive to all of the frequencies of the liquid turbulent velocity fluctuations. They are able to follow the low frequencies that dominate the streamwise velocity fluctuations, but not the high frequencies associated with the radial velocity fluctuations. As a result, extra dissipation of the radial velocity fluctuations occurs, and the radial velocity fluctuation levels are lowered. A similar reduction in the transverse velocity fluctuations has been observed in wall-bounded turbulent flows.[4,5]

There are a number of implications to the present measurements. First, any theoretical model of turbulence modulation must take into account the spectral response of the particles to realistically capture the attenuation effects. Second, seed particles used for LDV and particle image velocimetry applications need to be chosen carefully so that turbulence modulation effects are minimal. Third, the present measurements, although consistent with the findings of Gore and Crowe,[2] indicate the inadequacy of one parameter, the length scale ratio, to solely describe turbulence modulation effects. This length scale ratio is 0.005 and 0.0036 for the 64-μm particles and 0.01 and 0.015 for the 180-μm particles at $x/d = 60$ and 40, respectively, for present measurements. All of these values are less than 0.1, indicating a decrease in the fluid turbulence due to the particles according to the Gore and Crowe[2] criterion. However, the 64-μm particles did not cause any turbulence attenuation at all. Therefore, other parameters, such as the ratio of the particle time constant to the timescale corresponding to the peak energy in the fluid velocity fluctuation spectrum, might be needed in addition to the length scale ratio to describe the effects of particles on fluid turbulence.

IV. Conclusions

In summary, the turbulence modulation effects of particles of two sizes (64 and 180 μm) and initial mass loadings (1.1 and 2.3%) in an axisymmetric jet were investigated using DLDV. Experiments were conducted using a single-phase and four particle-laden turbulent jets. Results from the single-phase jet agreed well with the existing experimental data for air-in-air turbulent jets. The turbulence intensities of the 64-μm particle-laden jets were comparable to those of the single-phase jet. Thus, the 64-μm particles at low loadings could be used as tracer particles. Effects of turbulence modulation by the particles were observed in the jets laden with the 180-μm particles. The axial velocity fluctuations were not affected significantly;

the radial velocity fluctuations were considerably attenuated because the 180-μm particles could not follow the high frequencies involved in the radial velocity fluctuations.

References

[1]Al Taweel, A. M., and Landau, J., "Turbulence Modulation in Two-Phase Jets," *International Journal of Multiphase Flow*, Vol. 3, No. 2, 1977, pp. 341–351.

[2]Gore, R. A., and Crowe, C. T., "Effects of Particle Size on Modulating Turbulent Intensity," *International Journal of Multiphase Flow*, Vol. 15, No. 2, 1989, pp. 279–285.

[3]Schreck, S., and Kleis, S. J., "Modification of Grid-Generated Turbulence by Solid Particles," *Journal of Fluid Mechanics*, Vol. 249, 1993, pp. 665–688.

[4]Kulick, J. D., Fessler, J. R., and Eaton, J. K., "Particle Response and Turbulence Modification in Fully Developed Channel Flow," *Journal Fluid Mechanics*, Vol. 277, 1994, pp. 109–134.

[5]Sato, Y., Hishida, K., and Maeda, M., "Effect of Dispersed Phase on Modification of Turbulent Flow in a Wall Jet," *Journal of Fluids Engineering*, Vol. 118, No. 2, 1996, pp. 307–315.

[6]Chang, Y.-H., "Velocity Measurements in a Particle-Laden Round Jet Using Discriminator Laser Doppler Velocimetry," M.S. Thesis, School of Aerospace and Mechanical Engineering, Univ. of Oklahoma, Norman, OK, Jan. 1998.

[7]Parthasarathy, R. N., and Faeth, G. M., "Structure of Particle-Laden Turbulent Water Jets in Still Water," *International Journal of Multiphase Flow*, Vol. 13, No. 5, 1987, pp. 699–716.

[8]Muste, M., Parthasarathy, R. N., and Patel, V. C., "Discriminator Laser Doppler Velocimetry for Measurement of Liquid and Particle Velocities in Sediment-Laden Flows," *Experiments in Fluids*, Vol. 22, No. 1, 1996, pp. 45–56.

[9]Ahmed, S. A., Nejad, A. S., and Al-Garni, A. Z., "A Comparative Study of the Effects of LDV Velocity Bias in the Near Field of a Turbulent Free Jet," *Canadian Aeronautics and Space Journal*, Vol. 41, No. 4, 1995, pp. 179–184.

[10]Hussein, J. H., Capp, S. P., and George, W. K., "Velocity Measurements in a High-Reynolds-Number Momentum-Conserving, Axisymmetric, Turbulent Jet," *Journal of Fluid Mechanics*, Vol. 258, 1994, pp. 31–75.

A. K. Aggarwal
Associate Editor

Evolution Strategies for Film Cooling Optimization

Sibylle D. Müller,* Jens H. Walther,† and Petros D. Koumoutsakos‡
Swiss Federal Institute of Technology, ETH Zentrum, 8092 Zurich, Switzerland

Introduction

An evolutionary algorithm is implemented in a realistic automated design cycle of turbine blade film cooling. This design cycle involves the use of empirical formulas for the flow calculation and the use of a commercial software package for the simulation of the heat transfer problem. The overall process consists of an engineering multiobjective optimization problem with constraints. In this work we consider the solution of this problem in the context of an automated optimization cycle using evolution strategies. Evolution strategies[1] are robust, highly parallelizable, and suitable for optimizing multimodal functions without requiring gradient information. An evolution strategy with derandomized covariance matrix adaptation of the mutation distribution is chosen that accelerates the convergence rate of the scheme by adaptively incorporating earlier information.[2] It is shown to be advantageous in this problem when compared with an evolution strategy with isotropic mutation distribution and cumulative global step size adaptation. In film cooling, the coolant leaves the blade through rows of holes, forming a protective film on the outer surface of the blade, separating the hot gas from the metal. The design of the cooling configuration aims at both minimizing the coolant supply and achieving optimum cooling, while obeying certain engineering constraints. For the simulation of the cooling configuration, we compute the mass flow of the coolant and the surface temperature of the blade based on given external aerodynamic and thermal conditions for a two-dimensional blade geometry.

Received 27 August 1999; revision received 29 June 2000; accepted for publication 31 October 2000.

*Graduate Student, Institute of Computational Sciences.
†Research Associate, Institute of Computational Sciences.
‡Professor, Institute of Computational Sciences.

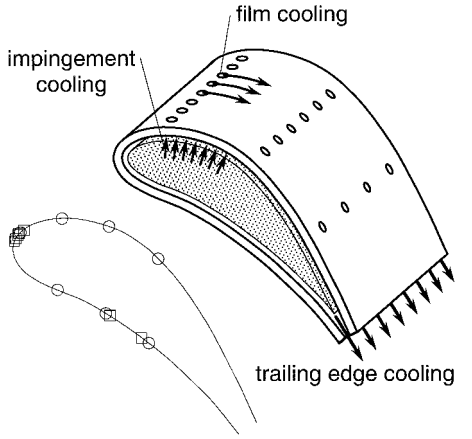

Fig. 1 Three cooling mechanisms and the initial (○) and final (□) row positions from the optimization with the CMA–ES.

Description of a Blade Cooling Configuration

A typical vane cooling configuration is shown in Fig. 1. It consists of three components: 1) an insert for impingement cooling, 2) the trailing-edge geometry for convection cooling, and 3) coolant air leaving the inside of the blade through holes and keeping attached as a film, thereby cooling the outer surface. The coolant flow is described by three different cooling mechanisms based on empirical correlations that compute the heat transfer coefficient and the temperature in the boundary layer.[3–5] The geometry and the external aerodynamic and thermal conditions are considered two dimensional, and the shape of the blade is fixed.

Blade Cooling Optimization

Optimization Algorithm and Parameters

The two chosen optimization techniques[2] are evolution strategies with intermediate recombination of all of the parents and with a population of 3 parents and 12 children, using strategy parameters according to Ref. 2. The first method is an evolution strategy with derandomized covariance matrix adaptation (CMA–ES), whereas the second method is an evolution strategy with isotropic mutation distribution and cumulative global step size adaptation (ES).

The optimization parameters are the number of film cooling rows R_f; the position of film cooling rows $s_{\text{pos}}(1-R_f)$; the injection angles of the holes, measured from the hole axis to the surface $\alpha(1-R_f)$; the number of holes per row $N_r(1-R_f)$; the number of impingement holes N_j; and the loss parameter that is a function of the pressure loss in the trailing edge A_{loss}.

The only integer parameter in the blade cooling optimization is the number of rows. Note that optimizing integer variables with an ES only makes sense if the number of possibilities to adjust the variables is large enough. Because of manufacturing requirements, the number of rows should not exceed about 10. With respect to this small number, this parameter is not included in the optimization process, but rather is changed manually for different optimization runs. First tries with $R_f = 4$ showed that the constraints for maximum and minimum temperature cannot be met. To homogenize the temperature distribution, we increased the number of rows to $R_f = 7$. This number was found to be sufficient for achieving the optimization goals and is used in this study.

All of the other parameters are real valued. For each film row $j = 1, \ldots, R_f$, the position s_{pos}, the angle α, and the number of holes per row N_r can be chosen. The other two parameters are the